*International Journal of Applied Mathematical Research*, 14 (2) (2025) 1-9

**International Journal of Applied Mathematical Research**

*Website: www.sciencepubco.com/index.php/IJAMR*
*https://doi.org/10.14419/1ct56h49*
***Research paper***

# Mathematical Modeling of a Solar Drier Temperature Profile

**Kenneth Korkoren *, Titus Rotich , Samwel Rotich**

*Moi University, School of Sciences and Aerospace Studies, Department of Mathematics, Physics, and Computing. P.O. Box 3900 – 30100, Eldoret, Kenya*
**Corresponding author E-mail: drtkchebion@gmail.com*

**Abstract**

Food shortages in most countries are not only associated with unfavorable weather conditions, but are also significantly blamed on ineffective post-harvest handling of food. Eminent threats caused by post-harvest losses due to inadequate drying and poor storage is responsible for up to 40-60% losses of agricultural produce each season. One of the mitigation strategies is the provision of sustainable and affordable food drying facilities. The most suitable solution is the use of solar food driers, which can be accessed locally. The optimal performance of a solar food drier depends on the consideration of design parameters and operation guidelines. This research paper models a solar drier to identify significant parameters and simulates to determine their optimal threshold values for the purpose of designing an effective solar drier suitable for dehydrating a variety of agricultural products. The model was formulated using a system of differential equations, to describe dynamics in four distinct compartments of a solar drier, namely; the solar heat collector, the closed loop pipe network circulating thermal fluid, the set of heat exchanger where heat is extracted from the hot liquid to hot drying air, and lastly is the dying chamber with controls of humidity, temperature, mass flow rate and energy balance. The set of solar dryer mathematical model equations was transformed to a MATLAB–SIMULINK model for simulation and parameter estimation. It was found that exposing a solar collector of $\eta_c$=0.8 efficiency, with aperture area of $A_c$=14.4m$^2$ and a fluid capacity of $V_c$=500l, to solar irradiation of average $I_c$=5.6637KW/m$^2$ can heat 5000 liters of water from $T_{in}$=22$^0$C to $T_{co}$=70$^0$C in 12 hours at a collector's flow rate of $\dot{v}_c$=1.128l/s. This heat energy in the thermal fluid can be extracted using a 5m$^2$ heat exchanger to obtain hot air of up to 70$^0$C, which can be regulated to the desired temperature depending on the food to be dried.

***Keywords***: *Solar Collector; Insolation; Mass Flow Rate; Convective Heat Transfer; Threshold Values.*

## 1. Introduction

Food is the most essential component to sustain the lives of living things. Food is a source of different types of nutrients, which when metabolized, play several roles in the body, including growth and development, protection from infections, energy, keeping our bodies warm, just to mention a few.

The major source of food for human consumption is from the food crops, whose production depends largely on the productivity of the soil and climatic conditions. The seasonality of weather also makes the production of food seasonal. There are seasons when food is produced in abundance, and there are seasons when food is scarce.

Due to the vast growing population, the demand for food and attempts to satisfy the demand are increasingly becoming a major concern globally. In Sub-Saharan Africa, food shortage is experienced by many people the tune of 70% of the total population. This has led to food shortages and fluctuations of prices due to seasonal production. According to [1]Over 10 million of the Kenyan population is facing acute food shortage due to food loss and waste. Over the years, the Kenyan government is trying to provide 51% of Kenyans who lack access to food due to a poverty index of 46% [2]. Kenya is an Agricultural country with 70% of the people depending on Agriculture as an economic activity. With a land mass of approximately 592,000 km2, only 20% is arable, and therefore, there is a need to optimize its use. In line with the Kenyan government's Vision 2030, food security is one of the priority areas outlined in the "Big Four Agenda" and the country has put in place necessary policies to enhance the production of food sufficient to feed over 45 million of its inhabitants [3]. The food loss is associated with insect and pest infestation (80 – 90%), humidity and growth of microorganisms (70%), and mycotoxins (25 – 40%) [4]. Food wastage and loss are over 1.3 billion tons globally per annum.

Due to a lack of homogeneity in the productivity of the land and differences in climatic conditions, some regions have insufficient production of food, while others have excess production, which leads to wastage. In order to balance the two regions, there is a need for perfect knowledge of market forces, demand, and supply, and an efficient system of conservation structures of perishable products. This calls for the need to conserve food to keep the food safe for consumption, nutritious, and of good quality between the time of production, during movement, to the time of use. Among the numerous causes of food waste, the major one is poor post-harvest management, which includes poor handling, moisture control, poor storage, and transportation, among others. Post-harvest loss is known to cause between 15% and 25% of the total food losses. Cereal grains alone account for the maximum post-harvest calorific basis losses up to 50 – 60%. The

major reason why food gets spoiled is because to decay [5]. Food decay due to microbial and biochemical processes is mainly catalyzed by the presence of moisture in the food substances [6]. All food products have moisture, and may be eaten fresh with the juicy content or when dry. Some foods, however, are meant to be eaten when dry. This is mostly plant seeds like cereals, but all the other food products can be dried to prolong their shelf life.

The major cause of this loss is associated with water activity and the growth of microbes, and the development of aflatoxins [7]. Water activity is the major contributor to microbial growth and the development of mycotoxins. Aflatoxin is known to be a group 1 carcinogen and the leading cause of liver diseases, anemia, poor appetite, and growth in humans and livestock. Drying of food reduces moisture to levels that cannot allow microorganisms to develop, thus making the food last longer without getting spoiled. This will enable the food to be stored for future use or to be transformed or processed. The food particles are made of a porous fixed skeletal matter, filled with moisture/water, and when dried to the desired moisture content, the water content is reduced and left with dry matter. Optimal drying of food products to achieve a threshold of less than 40% moisture content eliminates conditions favourable for the growth of secondary metabolites and therefore reduces damage to cereals and associated losses to less than 1% [4].

The methods of drying food products include: natural drying in the sun, use of electricity as a source of heat, or use of organic fuels. The cost involved in drying foodstuffs using electricity is enormous, and not all farmers can afford to meet the cost. The use of fuels, however, may be relatively cheap, but it has negatively on the environment. The use of solar energy is the cheapest option, but may lead to contamination if food products are dried in the open, on the road, or in fields. Most farmers dry their cereals in the open air, using canvas sheets. This will expose the food to unhygienic conditions, dust, grass, leaves, and wood particles, which make the food unclean. Through these indigenous methods, food is also exposed and eaten by birds and other animals, leading to losses.

It is for this reason that in this research study, we propose to analyze the design and operation of a solar food dryer, which can offer a clean environment for drying food products. The solar food dryer operates by using solar energy to heat water, which will then be used to dissipate heat using heat exchangers to the surrounding dry air. The hot air from the heat exchanger is then channeled into an enclosed drying chamber, where food products are placed to dry.

## 2. Solar energy and drying technologies

The ultimate source of heat energy is the sun. This is the natural source which is cost-free, and this energy can be transformed into other forms of energy depending on the requirements. The cost of using heat energy from the sun is met only in the process of collecting, transforming, and channelling it to the required place of use. The sun is made up of a ball of gases under pressure, and nuclear fusion changes hydrogen to helium, producing heat and light. The ball of huge hot gases (hydrogen gas (70%), helium (28%), carbon and oxygen (1.5%), and other gases making up to 0.5%), which are held together by the force of gravity, forming a spherical shape. Many other elements like neon, iron, silicon, magnesium, and sulphur are found in small quantities in the sun [8].

The temperature of the sun is about $5{,}700^0$C, and through insolation, the Earth receives this thermal energy from the sun. The Earth's surface is heated, and depending on the nature of the material, the elevation, and the location on the Earth's surface, the surface temperature varies. The highest recorded temperatures on the Earth's surface are: at $58^0$C in Africa, $54^0$C in Asia, 500°C in Europe, and as low as $15^0$C in Antarctica. Using solar photovoltaic cells, this radiation from the sun can be collected and converted for domestic use, which includes boiling water, heating rooms and drying chambers, and driving electrical machines.

The solar domestic hot water model studied is composed of the solar collector, storage tank, and the targeted greenhouse compartment, all interconnected with a series of insulated pipes ferrying hot and cold water. Heat and mass transfer equations were used in modeling the heat dynamics in a greenhouse. Block block-oriented approach was used in modeling domestic solar heating. Simulations were run for a period of 24 hours using MATLAB-SIMULINK, and the model results showed significant equivalence with the measured data. [9]. In this study, however, no heat exchangers were used.

As an intervention strategy for food security, studies on solar food drying technology were done by [10]. The study focused on a fully packed continuous conveyor direct-fired dryer. Food and drying air mass and energy balance equations were used to model the dryer. Simulation results were run to optimize the drying air velocity and temperature parameters. In this study, methane fuel was used as a source of energy, which heated the hot air circulation in the dryer. It was found that mass and energy transfer equations were able to model the drying process of the food particle. Model optimal operation was found to be closely equivalent to the experimentally measured data. In this model, the dryer is a directly heated continuous conveyor belt, with direct heating from burning methane gas.

Drying technologies of food were also studied by [11], [12]. In their study, various characteristics of food are discussed. These include physical and chemical changes experienced during drying. The effect of moisture, popularly known as water activity, is explored in detail. Various drying technologies and dehydration processes are discussed. The various modes of heating explored include: convectional heating, radiative heating, and microwave. Radio frequency and joule heating are explored.

A mathematical model of the drying process of skin and hides was studied by [13]. Two fundamental equations on heat and mass transfer were used to model the drying process. It was found that the transient distribution of moisture and heat in leather can be predicted and therefore optimized to conserve energy.

Studies on the drying process of vegetables were done by [14] using a rotary dryer. Air and product temperature and humidity were determined and compared with actual data measurements, and a significant correlation was found. Six differential equations were analyzed to solve and determine the optimal ranges of six parameters, which include inlet temperature, air flow rate, moisture loss rate, outlet air temperature, and humidity. From dynamic simulation, it was shown that the temperature and moisture content of the products and the drying air can be predicted and therefore determine the drying time required for each product. Inlet air temperature was found to be more significant in the drying process than the air flow rate in a parallel flow, but for concurrent flow, the air flow rate was found to be a significant component in the drying process [14].

The big question which this research study is trying to answer is, for how long, at what temperature, at what air flow rate and velocity, do a certain quantity of food products at a certain initial moisture content, is required to dehydrate but still maintain high quality final product to desired moisture content, and at what cost of energy. These are answered from the model to be formulated, and simulations to be run.

The results obtained in this study are not only helpful to other researchers as an indicator of the starting point for further research, but also provide the common man with an alternative optimal drying technology, which can be used both at the domestic and commercial level in drying food. The research study produced valuable information for the agricultural sector in the government, which is used to enhance the struggle to minimize food loss due to post-harvest challenges, and thus reduce hunger and access to food. The information is specifically on the threshold values of control parameters, which contribute to the construction of an optimal prototype food dryer. The

design of the solar food drier is environmentally friendly and in line with the global efforts to explore green energy and protect the environment.

## 3. Solar dryer model

In this section, the solar dryer model is described in terms of its components and their interrelation. The model is subdivided into four sections, namely, the solar collector system, the piping system, the heat exchanger system, and the drying compartment. The solar water heater, as the source of heat, gets a supply of water from a reservoir, pushed through a closed loop of pipes by a water pump. Cold water from the tank enters through the solar heater, collecting heat from the solar radiation, and the hot water is channeled back to the reservoir through the heat exchanger. The heat exchanger is designed to extract heat from the water to air, and the hot air is passed through the drying chamber at a controlled velocity, humidity, temperature, and direction of flow. The hot air is then expected to dry moist food in the drying chamber trays. The description is illustrated in Figure 1 below.

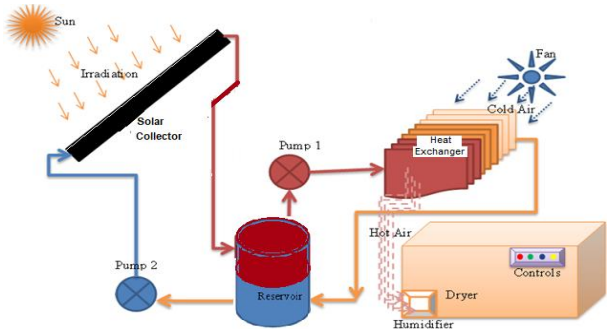


The heat energy and mass balance dynamics in the solar dryer are studied using mathematical equations. These equations were formulated for each section of the dryer and coupled to give the state of the entire system. However, model equations representing the solar and other alternative heat sources are analysed separately because of their independence from the other compartments. Once the solutions giving optimal heat from the solar collector are achieved, the output temperature profile solution is used as the input fluid temperature in the other compartments. After considering heat losses, the output of the piping system becomes the input to the heat exchanger, which is then used to determine the drying hot air temperature profile.

### 3.1.1. Mathematical equations of the solar collector

The solar collector is made up of several glass tubes arranged and interconnected to form a rectangular-shaped solar collector, where water flows in, gets heated, and the hot water flows out at a given flow rate determined by a water pump connected to the source. Forty-eight solar collectors are arranged in four rows and twelve columns, each made up of a system of 100 tubes measuring 32mm in diameter and 1000mm long. A metal frame measuring 13m by 4m is fabricated to hold the solar collectors inclined at $45^0$ degrees, facing eastwards, to collect as much radiation from the sun as possible.

The equations describing the working and the efficiency of the solar collector are formulated using ordinary differential equations and solved both analytically and numerically. The components of this subsystem include the solar irradiation, solar collector panel, and the tubes where the fluid flows. Parameters like solar efficiency, flow rate, input and output temperatures of the fluid together with the ambient temperature of the solar collector were utilized.

Using conservation equations, the differential equation accounting for the net change in heat energy in the solar collector is given as follows. Let the input flow rate of water into the collector at a temperature of $T_{ci}$ degrees celsius be given by $\dot{v}_{ci}$, let the flow rate out of the collector be $\dot{v}_{co}$, with the assumption that $\dot{v}_{ci} = \dot{v}_{co}$ and let the output water temperature be $T_{co}$. Also, let $T_{ca}$ be the ambient air temperature around the collector, while $I_c$ and $U_c$ be the irradiance on the collector plate in $W/m^2$ and overall heat loss coefficient respectively. The differential equation accounting for the change in output temperature of the fluid is given by;

$$\frac{dT_{co}}{dt} = \frac{A_c \eta_c I_c}{\rho_c c_c V_c} - \frac{U_c A_c}{\rho_c c_c V_c}(T_{av} - T_{ca}) + \frac{\dot{v}_c}{V_c}(T_{ci} - T_{ca}) \tag{1}$$

Where $\eta_c$, is the solar collector's efficiency, the aperture surface of the collector is $A_c$, density of the collector fluid is $\rho_c$, volume of the collector fluid $V_c$, the average fluid temperature in the collector is [15].

$$T_{ca} = 0.5(T_{ci} + T_{ca}) \tag{2}$$

According to the analysis of performance of solar collector done by [16], the solar collector efficiency $\eta_c$ is evaluated as

$$\eta_c = \eta_0 - a\frac{(T_{av} - T_{ca})}{G} - b\frac{(\bar{T} - T_a)^2}{G} \tag{3}$$

Where $\eta_0$ is the manufacturer's rated efficiency, $a, b$ are solar collector constants, $T_{av}$ is the average temperature in the collector. From the experimental analysis done by [16], the efficiency of the glass evacuated vacuum tube was found to be

$$\eta_c = 0.536 - 0.8240\frac{T_{av} - T_{ca}}{I_c} - 0.0069\frac{(T_{av} - T_{ca})^2}{I_c} \tag{4}$$

The average solar radiation emitted by the sun is known to reach the outer atmosphere, called the solar constant is at the rate of about 1.367 kW/m$^2$ , and the total emission of the sun is about 3.7× 10 W/s. [17]. This radiation may be divided according to its spectral distribution into UV, visible and near IR, the latter two accounts for about 90% of the total emission [18]. The atmosphere distorts the solar

radiation and alters the wavelength distribution, and therefore the solar energy actually reaching the ground varies with latitude, season, time of day and other factors such as topography, meteorological elements, atmospheric dust and contamination. The radiation available on the ground is composed of beam or direct radiation and diffuse radiation, producing half of the available energy.
For the purpose of this research, irradiation data collected in Nairobi, Thika and Dagoreti towns in Kenya were acquired from [19], [20] and presented in Table 1.

**Table 1:** Insolation Data Collected for 12 Hours in Dagoreti, JKIA and Thika. [19]

| Thika, Dagoreti and Jomo Kenyatta Airport Average | | | | | | | | | |
|---|---|---|---|---|---|---|---|---|---|
| TIME | kWh/m$^2$ | TIME | kWh/m$^2$ | TIME | kWh/m$^2$ | TIME | kWh/m$^2$ | TIME | kWh/m$^2$ |
| 6:30 AM | 3.15 | 9:00 AM | 12.45 | 11:30 AM | 19.4 | 2:00 PM | 11.15 | 4:30 PM | 7.15 |
| 6:40 AM | 4.55 | 9:10 AM | 13.2 | 11:40 AM | 18.65 | 2:10 PM | 11.05 | 4:40 PM | 6.85 |
| 6:50 AM | 5.7 | 9:20 AM | 14.1 | 11:50 AM | 18.05 | 2:20 PM | 10.7 | 4:50 PM | 6.6 |
| 7:00 AM | 5.7 | 9:30 AM | 15.7 | 12:00 PM | 17.25 | 2:30 PM | 10.55 | 5:00 PM | 6.8 |
| 7:10 AM | 5.6 | 9:40 AM | 16.85 | 12:10 PM | 16.55 | 2:40 PM | 10 | 5:10 PM | 6.4 |
| 7:20 AM | 5.6 | 9:50 AM | 17.8 | 12:20 PM | 16 | 2:50 PM | 9.7 | 5:20 PM | 6.4 |
| 7:30 AM | 5.65 | 10:00 AM | 18.55 | 12:30 PM | 15.35 | 3:00 PM | 9.3 | 5:30 PM | 6.3 |
| 7:40 AM | 5.7 | 10:10 AM | 19 | 12:40 PM | 14.75 | 3:10 PM | 9.15 | 5:40 PM | 6.25 |
| 7:50 AM | 6.15 | 10:20 AM | 19.55 | 12:50 PM | 14.15 | 3:20 PM | 8.95 | 5:50 PM | 6.2 |
| 8:00 AM | 6.65 | 10:30 AM | 19.7 | 1:00 PM | 13.7 | 3:30 PM | 8.85 | 6.00 PM | 6.0 |
| 8:10 AM | 8.4 | 10:40 AM | 20 | 1:10 PM | 13.35 | 3:40 PM | 8.4 | 6.10 PM | 3.55 |
| 8:20 AM | 8.9 | 10:50 AM | 19.95 | 1:20 PM | 12.85 | 3:50 PM | 8.1 | 6.20 PM | 3.15 |
| 8:30 AM | 10.3 | 11:00 AM | 19.8 | 1:30 PM | 12.55 | 4:00 PM | 7.95 | 6.30 PM | 2.3 |
| 8:40 AM | 10.95 | 11:10 AM | 19.75 | 1:40 PM | 12.25 | 4:10 PM | 7.55 | | |
| 8:50 AM | 11.55 | 11:20 AM | 19.65 | 1:50 PM | 11.55 | 4:20 PM | 7.35 | | |

### 3.1.2. Analytic solution of solar equation

The analytic solution of the solar collector equation (1) is obtained by separation of variables and integration method.
Let $\alpha = \frac{A_c\eta_o I_c}{\rho_C c_c V_c} - \frac{U_c A_c}{2\rho_C c_c V_c}T_{ci} + \frac{U_c A_c}{\rho_C c_c V_c}T_{ca} + \frac{\dot{v}_c}{V_c}T_{ci}$, and let $\beta = \left[\frac{U_c A_c}{2\rho_C c_c V_c}T_{co} + \frac{\dot{v}_c}{V_c}\right]$, then the equation above reduces to; $\frac{dT_{co}}{dt} = \alpha - \beta T_{co}$ whose solution is obtained by separation of variables to be;

$$T_{co}(t) = \alpha\beta\left(1 - e^{-\beta t}\right) + T_{ci}e^{-\beta t} \tag{5}$$

Note that the limit as $t \to \infty$ equation (5) yields the steady state temperature obtained at prolonged exposure of the solar collector to constant irradiation, given by; $T_{co}(t) = \alpha\beta$

### 3.1.3. Piping system mathematical model equations

In order to describe the dynamics of heat transfer along the pipes, it is necessary to consider the effect of parameters like insulation, type of material, length of pipes, diameter, mass flow rate among others. The temperature of the water from the collector is taken to be $T_{co}$ and as water flows through pipes, the heat may be lost through two processes; Conduction and/or Convection or both. The mathematical equations describing the conductive and convective heat loss are explained below.
Heat loss is experienced when the pipe, which is in contact with the water is heated, and thus the water loses heat energy to the pipe material, as it flows along the pipe. This heat loss can be reduced by using a material with less heat conductivity coefficient or by thickening the walls of the pipes using insulators. From experimental tests, some materials have a known conductivity coefficient, for example steel has $45W/mK$, while copper has $398W/mK$, Aluminium $205W/mK$, Glass $0.8W/mK$ and Polystyrene $0.03W/mK$. From these values, it means that copper conducts heat faster and more effectively than steel [15].
In this paper, optimal heat loss is targeted by choosing a material or modifying piping material through insulation, so that heat energy in the fluid from the solar collector reaches the heat exchanger with minimum or no losses. This ensures that maximum heat is extracted from the water to the drying air.
The following are the mathematical equations describing the heat loss through conduction and convection in the piping system.
The conductive heat transfer is given by the formula

$$Q_{cond} = \frac{kA(T_{ci} - T_\infty)}{d} \tag{6}$$

Where k is the thermal conductivity, A is the surface area of the material, $T_\infty$ is the temperature of the surrounding environment and d is the thickness of conducting material. On the other hand, convective heat loss is defined by the formula

$$Q_{conv} = h_{conv}A(T_p - T_\infty) \tag{7}$$

Where $h_{conv}$ is the convective heat transfer coefficient, and $T_p$ is the temperature of the pipe surface.
A measure of all the components contributing to heat loss is represented by the ability of the material to resist heat loss. The thermal resistance of a pipe is given by the formula;

$$R_{cond} = \frac{\ln\left(\frac{r_0}{r_i}\right)}{2\pi kL} \tag{8}$$

Where $R_{cond}$ (in K/W) is the thermal resistance of the pipe, $r_0$ is the outer radius of the pipe, $r_i$ is the inner radius of the pipe, L is the length of the pipe and k is the thermal conductivity. Similarly, the convective heat resistance $R_{conv}$ (in K/W) is given by;

$$R_{conv} = \frac{1}{kA} \tag{9}$$

While the radiative thermal resistance is also given by

$$R_{rad} = \frac{T_p - T_\infty}{\varepsilon A \sigma (T_p^4 - T_\infty^4)} \tag{10}$$

Here, the parameters ε denotes the radiative coefficient, σ conductivity and $A_s$ is the surface area.
The total resistance of the material is therefore given by;

$$R_{tot} = R_{cond} + R_{conv} + R_{rad} \tag{11}$$

This is obtained from finding the total sum of equation (8 - 10).
The total heat loss in the piping system is computed as;

$$Q_{tot} = \frac{\Delta T}{R_{tot}} = UA\Delta T \tag{12}$$

Where $U = \frac{1}{R_{tot}A}$ is the total thermal coefficient, and ΔT is the temperature difference between the fluid and the surrounding environment.
From the above equations, the output temperature $T_{co}$ can be calculated at the end of the pipe system, to determine the output temperature at the point where the pipe enters the heat exchanger. This is given by;

$$T_{out} = T_t + (T_{out} - T_t)e^{-\frac{4h}{c_p \rho v D}x} \tag{13}$$

This is the piping system output temperature expected at the heat exchanger's input point, equivalent to equation (5).

## 3.2. Solar drier model simulation

This section presents detailed analytic and numerical results of the solar drier model under study. These results are presented in various sections, subdivided into two categories, namely; Solar drier mathematical model equations and their analysis, where all the simulation is done using MATLAB – SIMULINK.
Mathematical equations, describing the collection of radiation from the sun, and heating the fluid in the solar collector pipe loop was modeled using equation (1). The analytic solution in equation (5) is compared with simulation results generated from SIMULINK.

### 3.2.1. Solar collector Simulink model and parameters

In order to carry out simulation of the performance of a solar collector, SIMULINK building blocks were arranged to represent the model in equation (1). The parameters involved in equation (1) include; area of the solar collector ($A_c$), fluid temperature into $T_{ci}$, and temperature out of the solar collector $T_{co}$, ambient temperature $T_{ca}$, mass flow rate $\dot{v}_c$, volume of the fluid in the collector $V_c$, irradiance data $I_c$, and heat loss $U_c$.
Parameter values used in simulation are listed in Table 2.

**Table 2:** Parameters for Solar Collector Heat Simulation

| Symbol | Parameter name | Value |
|---|---|---|
| $\mathbf{A_c}$ | Solar collector Aperture area | 14.4m$^2$ |
| $\mathbf{V_c}$ | Volume of the fluid in the collector | 500 |
| $\dot{\mathbf{v}}_\mathbf{c}$ | Fluid velocity into the collector | variable |
| $\mathbf{T_{ci}}$ | Collector fluid input temperature | 22$^o$C |
| $\mathbf{T_{co}}$ | Collector output fluid temperature | Unknown |
| $\mathbf{T_{ca}}$ | Ambient temperature of the collector | 27$^o$C |
| $\mathbf{U_c}$ | Average heat loss in the collector | 7W/m$^2$K |
| $\mathbf{I_c}$ | Irradiance data of solar energy | Table 1 |
| $\boldsymbol{\rho}_\mathbf{c}$ | Density of the fluid in the collector | 1000 |
| $\mathbf{C_c}$ | Specific heat capacity of thermal fluid | 997 |
| $\boldsymbol{\eta}_\mathbf{c}$ | Solar collector efficiency | 0.87 |
| $\mathbf{T_{av}}$ | Average temperature, $\frac{1}{2}(T_{ci} + T_{co})$ | Calculated |
| $\mathbf{C}$ | Heat capacity of the fluid in KJ/Kg $^0$C | 4.186 |

The SIMULINK model for a solar collector is presented in Figure 2. Irradiation data in Table 1 is fed into the SIMULINK network, and with variation of the velocity $\dot{v}_c$, area $A_c$ and the volume of the collector, the output temperature $T_{co}$ is obtained. Three inputs, namely; input temperature, ambient temperature and solar irradiation are fed into the SIMULINK model, and one output (the fluid output temperature) is measured. It is noted that the output temperature keeps on increasing because of continued heating and reheating of the fluid. It is noted that the total cumulative temperature of the thermal fluid reaches 101.54$^0$C in 3 days. The output heat energy in the thermal fluid is sufficient to be dissipated to the drying air via the heat exchanger, in the drying chamber.

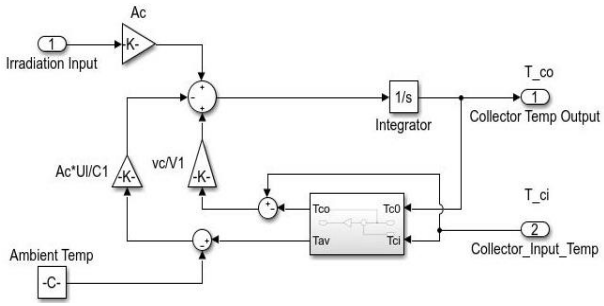


**Fig. 1:** SIMULINK Model of a Solar Collector.

### 3.2.2. Solar collector simulation

Using the solar irradiation data provided in Table 1, the simulation results of the solar collector is presented below. It is noted that as the velocity of the fluid is inversely proportional to collector's output temperature, but input temperature, ambient temperature and the aperture surface area, are directly proportional to the output temperature of the fluid. The desired output temperature is between $343\text{K}\ (70^0\text{C})$ and $423\text{K}\ (150^0\text{C})$, and for this, the optimal mass flow rate is $[500 - 1025]\text{cm}^3/\text{s}$. Note that the cumulative fluid output temperature reaches $60^0$ C after 1 day and keep increasing to a stable temperature of approximately $130^0$C after 10 days as shown in Figure 3 below.

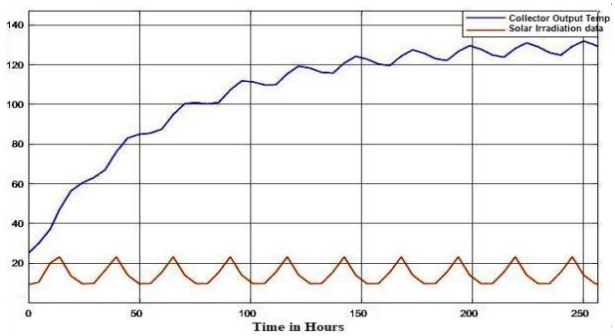


**Fig. 2:** Solar Irradiation Temperature and Cumulative Fluid Temperature Out of Collector.

## 3.3. The piping system

Modelling the piping system involves specifying parameters that describe the parameters of the pipes used in the model. These includes the length, diameter, internal and external surface area, insulation, heat conductivity, density, and specific heat capacity of the pipe material. The SIMULINK block that models pipe flow dynamics in a thermal liquid network due to viscous friction losses and convective heat transfer with the pipe wall is presented in **Error! Reference source not found.**4.

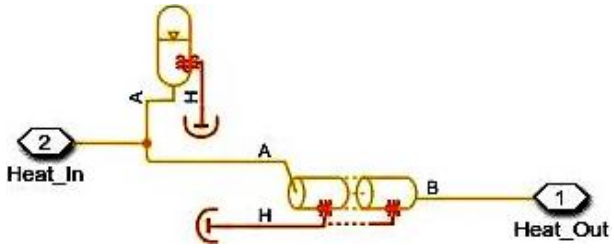


**Fig. 3:** SIMULINK Pipe Network.

The ports A and B are the thermal liquid conserving ports representing the pipe inlet and outlet points, The piping network is also connected to an insulated gas filled accumulator, which acts as a pressure balancing mechanism to minimize the possibility of pipes bursting due to build in pressure as a results of heating. In this study, a total of 10m length of pipe is used, with internal diameter of 0.02m and placed with zero inclination. The flow is assumed to be laminar with Nusselt number for laminar flow heat transfer of Nu = 3.66. The total heat loss along the pipe network is evaluated as the sum of heat loss due to conduction, radiation, and convection. The output temperature at the end of the pipe is computed using equation (13). From the simulation results, the temperature of fluid inside the pipe remains constant throughout as per the input temperature. This is a condition of perfect insulation.

## 3.4. The heat exchanger

The heat exchanger is the device which aids in the exchange of heat energy between two fluids. In this study, heat is extracted from thermal fluid (water) inside the closed loop pipe network out to the drying air (gas) blown across the exchanger by fans in the drying chamber. Countercurrent heat exchanger is chose to maximize the output temperature. The temperature of this output hot air is regulated by a set of fans, using mass flow rate and appropriate combination with relatively cold air from the environment. The physical representation of countercurrent heat exchanger is given in Figure 5.

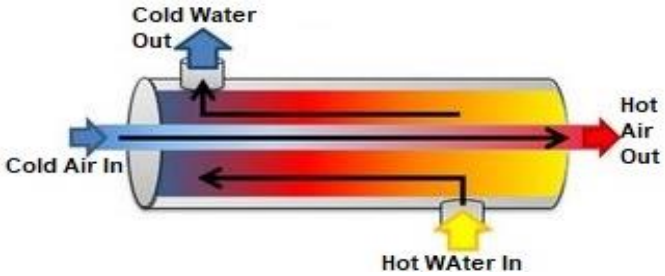


**Fig. 4:** Countercurrent Model of Liquid to Gas Heat Exchanger.

### 3.4.1. SIMULINK network of heat exchanger

The SIMULINK network flow of heat exchanger is represented in Figure 6 below. This SIMULINK block models a heat exchanger, where the heat transfer rate is based on the number of transfer units (NTU). In our model, the two fluids used was water and air (TL-G). Hot water from the solar heater passes through the heat exchanger, and transfer the heat to air, which is then channeled to the drier to heat and dry the food particles.

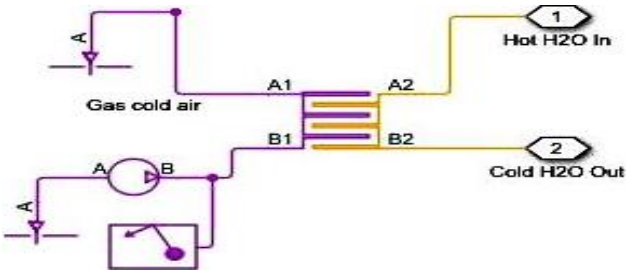


**Fig. 5:** Countercurrent Heat Exchanger SIMULINK Model.

Ports A2 and B2 in the heat exchanger SIMULINK network are the thermal liquid inlet and outlet. The inlet A2 describes the flow of hot water from the solar collector, and the outlet B2 represents the flow out from the heat exchanger. The cooled water flows back to reservoir tank, then pumped through another cycle of solar heating. Ports A1 and B1 is associated with the inlet and outlet of the controlled fluid, in this case cold air. The cold air flows from port B1 to A1, countercurrent to the flow of the hot liquid, so as to pick the maximum heat from the water. The source of the cold air is the environment, but passing through a humidifier to ensure that the inlet air is dry. This air is expected to be at environmental temperature, of $20^0$C on average, and leaves the heat exchanger by a forced air mass flow using a fan, at a temperature higher, depending on velocity and temperature of the thermal liquid in the exchanger. The total of 7.67m of the thin flat pipe is folded severally so as to increase the surface area.

### 3.4.2. Temperature simulation in the heat exchanger

The output temperature of air across the heat exchanger is plotted in Figure 7 below. The temperature is recorded without regulation at various air mass flow rate as indicated in the graph. Temperature controls is done by varying the mass flow rate, varying the number of heat exchangers operating, or blowing in cold air to lower the drying chamber temperatures.
The temperature profile of hot air from the heat exchanger is plotted in Figure 7, at different air mass flow rates.

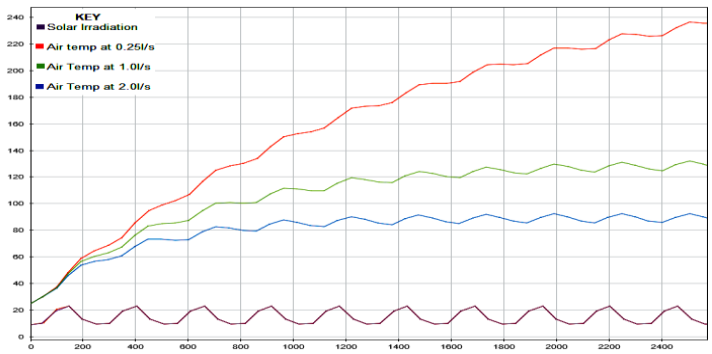


**Fig. 6:** Output Temperature of the Hot Air from the Heat Exchanger at Different Air Mass Flow Rate.

## 3.5. Food drying chamber

The next subsystem in the model is the drying chamber. This is the final and major target of the entire model, where food products to be dried are placed in trays in the drying chamber, and once the door and windows are sealed appropriately, switched are put on to allow hot dry air in and to eliminate moist air in the drier. Measuring devices are placed to monitor the temperature, time, mass flow rate, number of radiators switched on, among others. The other subsystems are adjusted to suit the requirements of the drying chamber. It is in the drying chamber that food products are placed, and exposed to hot drying air for dehydration depending on their nature. Various food products that need to be dehydrated have their upper limit of maximum temperature that can be exposed to dehydrate, of which, beyond this limit, the food products will start getting cooked or roasted, thus spoiling their quality. Table 3. shows desired dehydration temperature ranges for different food products [21].

**Table 3:** Dehydration Temperature Ranges of Food Products[21]

| | Food Type | Temp (°C) |
|---|---|---|
| 1 | Apples | 57–63 |
| 2 | Bananas | 57–63 |
| 3 | Berries | 50–57 |
| 4 | Grapes (Raisins) | 57–63 |
| 5 | Tomatoes | 57–63 |
| 6 | Carrots | 57–63 |
| 7 | Potatoes | 60–65 |
| 8 | Onions | 57–63 |
| 9 | Spinach | 50–57 |
| 10 | Peppers | 57–63 |
| 11 | Corn | 57–63 |
| 12 | Rice | 60–65 |
| 13 | Wheat | 60–65 |
| 14 | Oats | 60–65 |
| 15 | Meat (Jerky) | 68–74 |
| 16 | Fish | 60–63 |
| 17 | Indigenous Vegetables | 35–45 |

### 3.5.1. Drying chamber components

The drying chamber contains 5 heat exchangers placed on the walls of the drying chamber; each fitted with controlled fans, to regulate the air mass flow rate, and also fitted with thermometers and mass flow rate devices to control the drying parameters. Food type, amount of food to be dried, their initial moisture content, the required final moisture content, and the expected urgency of the drying process (or residence time) determines the adjustment to be done on the dryer [22]. These adjustments are made on the hot air mass flow rate, thermal liquid mass flow rate, number of radiators in use, and the opening and closing of ventilation windows to control the energy and moisture content, depending on the needs of food product information in Table 3.

**Table 4:** Drying Chamber Simulation Parameters

| No | Symbol | Description | value |
|---|---|---|---|
| 1 | $h_{air,wall}$ | Convective heat transfer coefficient (average) | 24 $\mathbf{W/m^2K}$ |
| 2 | $A_{s,wind}$ | Area of each squared windows | 0.25 $\mathbf{m^2}$ |
| 3 | $A_{s,roof}$ | Area of the roof | 14.4 $\mathbf{m^2}$ |
| 4 | $A_{s,wall}$ | Area of the walls | 40.32 $\mathbf{m^2}$ |
| 5 | $\rho_{wall}$ | Density of the walls (drier wall, floor and roof material) | 1920 $\mathbf{Kg/m^3}$ |
| 6 | $\rho_{wind}$ | Density of the window | 2700 $\mathbf{Kg/m^3}$ |
| 7 | dim | Dimensions of the drier chamber (l × w × h) | $\mathbf{6 \times 4 \times 2.4\ m}$ |
| 8 | No | Number of windows in the drier and radiators | 5 |
| 9 | $h_r$ | Radiative (radiator) heat transfer coefficient | 100 $\mathbf{W/m^2K}$ |
| 10 | $h_{air,roof}$ | Convective roof - Atmosphere heat transfer coefficient | 38 $\mathbf{W/m^2K}$ |
| 11 | $A_{s,rad}$ | Surface area of each radiator | 1$\mathbf{m^2}$ |
| 12 | $k_{wind}$ | Thermal conductivity of the window | 0.78 $\mathbf{W/mK}$ |
| 13 | $h_{air,wall}$ | Convective wall - Atmosphere heat transfer coefficient | 34 $\mathbf{W/m^2K}$ |
| 14 | $\mathbf{h_{air,wind}}$ | Convective window - Atmosphere heat transfer coefficient | 32 $\mathbf{W/m^2K}$ |

## 4.5. Drying chamber temperature simulation

Simulation of energy dynamics in the subsystems making up the solar drier is presented in this subsection. Temperature profile of dry air in the drying chamber at any time is plotted. This simulation is done for a dehydration temperature of $63^0$C. The controls can be automated so that a drop is temperature due to cooling by evaporating moisture from the food is compensated by raising the output temperature from the heat exchanger. In the graphs presented, the target was to maintain a hot drying air temperature of $63^0$C circulating the chamber. The solar irradiation, the thermal fluid temperature and the hot air temperature profiles are all plotted on the same graph using simulation parameters presented in Table 4. The temperature profile of thermal fluid in the radiator and the temperature of hot drying air are simulated in Figure 8.

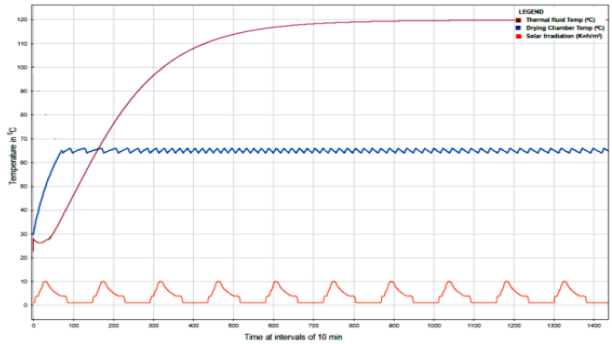


**Fig. 7:** Drying Chamber Temperature Profile, Solar Irradiation and Thermal Fluid Temperature

The temperature profile of hot drying air in the food chamber is regulated to fit the requirement of the type and the moisture content of the food to be dried. A constant drying chamber temperature of $65^0$C is illustrated in Figure 8.

## 4. Conclusion

The use of solar energy to dry food as a mitigation strategy for food security is simulated in this research and the findings indicate that; with the Kenyan solar insolation of between $5.4\text{KWhr/m}^2$ and $20.50\text{KWhr/m}^2$ , the use of solar collector with efficiency of $\eta_c = 80\%$ is able to collect solar thermal heat and heat $5000\text{l}$ of water from $22^0\text{C}$ to $101.54^0\text{C}$ in 36 hours, at a mass flow rate of $1.128\text{l/s}$. This energy can be extracted using heat exchangers to generate hot drying air of between is amazing energy that can be harvested and used for other purposes, including heating swimming pools, heating cooking water, heating water for domestic use, among others.
In this research, the same energy in the hot water was channeled to a heat exchangers, containing a loop of 7.66m pipe, of radius $\text{r} = 0.02\text{m}$, and a heat transfer coefficient of $100\text{W/m}^2\text{K}$. It was found that the hot air blowing through the heat exchanger is heated to between $90^0\text{C}$ and $130^0\text{C}$ depending on the flow rate. This hot air is regulated to desired temperature and passed through a humidifier and to the food drying chamber, for a period of time depending on the food moisture content, volume, and desired residence time.
Alternative energy sources may be used to heat the water so as to supplement the solar insolation, especially during cloudy seasons and at night. Other non-corrosive fluids with higher specific heat capacities can be used instead of water in the model.

## Acknowledgement

I acknowledge the guidance of my supervisors and the contribution of energy experts in improving the quality of this research. The use of solar irradiation data, and MATLAB Simulink Library blocks is also acknowledged.

## References

[1] Zhongming, Z., et al., Food loss and waste must be reduced for greater food security and environmental sustainability. International Journal of food nutrition and safety, 2020.
[2] Kiome, R., Food security in Kenya. Nairobi: Ministry of Agriculture, Kenya, 2009.
[3] Njura, H.J., I.K. Kaberia, and S.T. Taaliu, Effect of agricultural teaching approaches on skills development for food security: a case of secondary schools in Embu County, Kenya. The Journal of Agricultural Education and Extension, 2020. 26(3): p. 239-252. https://doi.org/10.1080/1389224X.2019.1680401.
[4] Kumar, D. and P. Kalita, Reducing postharvest losses during storage of grain crops to strengthen food security in developing countries. Foods, 2017. 6(1): p. 8. https://doi.org/10.3390/foods6010008.
[5] Rawat, S., Food Spoilage: Microorganisms and their prevention. Asian journal of plant science and Research, 2015. 5(4): p. 47-56.
[6] Veld, J.H.H., Microbial and biochemical spoilage of foods: An overview. International journal of food microbiology, 1996. 33(1): p. 1-18. https://doi.org/10.1016/0168-1605(96)01139-7.
[7] Kumar, P., et al., Aflatoxins: A global concern for food safety, human health and their management. Frontiers in microbiology, 2017. 7: p. 2170. https://doi.org/10.3389/fmicb.2016.02170.
[8] Asplund, M., et al., The chemical composition of the Sun. arXiv preprint arXiv:0909.0948, 2009.
[9] Buzás, J. and I. Farkas. Solar domestic hot water system simulation using block-oriented software. in The 3rd ISES-Europe Solar Congress (EuroSun 2000), Copenhagen, Denmark. 2000.
[10] Neto, A.N., Dryer modeling and optimization. 1997, Texas Tech University.
[11] Chen, X.D. and A.S. Mujumdar, Drying technologies in food processing. 2009: John Wiley & Sons.
[12] Xiao, D., C and S. Arun, M, Drying Technology and Food Processing. International Journal of food nutrition and safety, 2008.
[13] Haghi, A., A Mathematical Model of theDrying Process. Acta Polytechnica, 2001. 41(3). https://doi.org/10.14311/226.
[14] Iguaz, A., et al., Mathematical modelling and simulation for the drying process of vegetable wholesale by-products in a rotary dryer. Journal of food engineering, 2003. 59(2-3): p. 151-160. https://doi.org/10.1016/S0260-8774(02)00451-X.
[15] Patterson, J.E. and R.J. Miers. The thermal conductivity of common tubing materials applied in a solar water heater collector. in 46th ASC Annual International Conference. Wenthworth Institute of technology. 2010.
[16] Budihardjo, I. and G. Morrison, Performance of water-in-glass evacuated tube solar water heaters. Solar Energy, 2009. 83(1): p. 49-56. https://doi.org/10.1016/j.solener.2008.06.010.
[17] Carbonell, D., J. Cadafalch, and R. Consul, Dynamic modelling of flat plate solar collectors. Analysis and validation under thermosyphon conditions. Solar Energy, 2013. 89: p. 100-112. https://doi.org/10.1016/j.solener.2012.12.014.
[18] Eltbaakh, Y.A., et al., Measurement of total and spectral solar irradiance: Overview of existing research. Renewable and Sustainable Energy Reviews, 2011. 15(3): p. 1403-1426. https://doi.org/10.1016/j.rser.2010.10.018.
[19] Wasike, N.W., Assessment of the solar radiation potential of the Thika-Nairobi area, panel sizing and costing. 2015.
[20] Ng'ethe, J., Performance Optimization of a Thermosyphon Flat Plate Solar Water Heater. 2019, JKUAT-COETEC.
[21] Vega-Mercado, H., Dehydration of foods. 2013: Springer Science & Business Media.
[22] Blog, D., Dehydrating Time & Temperature Guide: Fruits, Vegetables, Meat, Herbs, Spices & Leather. 2018.